A TRANSVERSE WIGGLER MAGNET FOR ADONE

M.Bassetti, A.Cattoni, M.Preger and S.Tazzari
INFN, Laboratori Nazionali di Frascati, 00044 Frascati (Italy)

A.Luccio
Università degli Studi di Pisa, 56100 Pisa (Italy)

Introduction

In the last few years, the installation of wiggler magnets on electron storage-rings has been proposed by several authors for two main purposes:

a) beam size and polarization control, to improve the performance of colliding beam machines[1,2];
b) synchrotron light radiation enhancement and shift of its critical wavelength towards higher energies[3].

It is a fact however that not enough experimental information is available.

The conventional transverse wiggler, whose installation on Adone is here proposed, has been conceived to provide the following performances and opportunities.

a) lowering of the synchrotron radiation critical wavelength from 8.3 Å to 4.6 Å, i.e. to the value that would be obtained if the ring could be operated at 2 GeV. (Source intensity could also be increased by a factor of up to 4). The expected synchrotron light spectrum at 1.5 GeV is given in Fig. 1;
b) detailed study of the effects on beam dimensions and damping rates (possibility of increasing the injection rate into the ring);
c) possibility, by later addition of a second wiggler, of a substantial increase in luminosity at low energy, in two of the present four interaction regions; at a limited cost and with the possibility of fast commissioning since a free straight section is available and it is planned to power the magnet from existing power supplies.

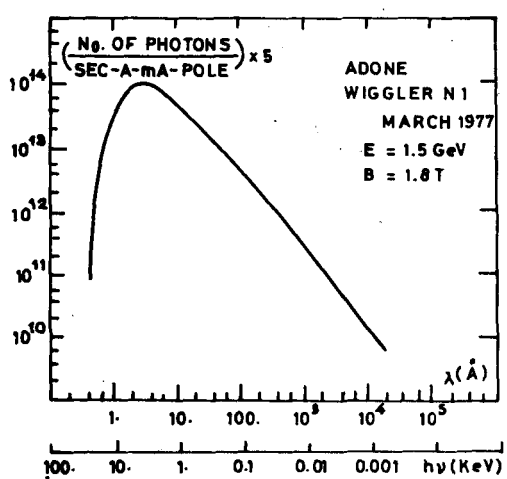

Fig. 1.

1. Magnet design

The wiggler magnet will be installed in one of the four available 2.5 m long interaction straights of Adone, with the field in the vertical plane (B = (0, 0, Bz)).

Taking into account the requirement that in the present mode of operation the beams be vertically separated by ~14 mm in all straights at injection (300 MeV), one finds that the equivalent aperture required at the wiggler (β_z = 3.8 m) is

$$a_{ss} \simeq 37 \text{ mm} .$$

Given this requirement, a round figure of 40 mm has been specified for the magnet gap, leaving an available aperture of ~35 mm instead of the computed 37 mm. With careful alignment of the magnet and possibly a better vertical closed orbit correction, we believe that normal machine operation will still remain practically unaffected.

Anyway the magnet is so designed that, if necessary, the aperture can easily be increased at the expense of a decrease in the maximum field. The proposed aperture is also compatible with operation in the colliding beam mode with two wigglers.

The design aims are:
- 6 full poles ,
- Max field 18 KG,
- Useful horizontal aperture at 10 KG: 200 mm + space required for trajectory inside wiggler.

The useful aperture is defined as the region where $\Delta B/B_0 \leq 10^{-3}$.

The constraints are:
- Existing power supply output: 400 V d. c., 5000 A ,
- Existing cooling system pressure: 6 atm at the magnet manifolds ,
- Gap height h $\geq$ 40 mm (due to the vertical aperture needed by the machine) ,
- Overall length $\leq$ 2300 mm .

The mechanical and main dimensional specifications of the magnet are summarized in Table I.

TABLE I. Magnet specifications.

Number of poles	5 full poles, 2 half poles
Gap height	40 mm
Pole width	280 mm
Field at center of gap	18 KGauss
Iron saturation at the yoke	$B_y \leq 15$ KGauss
Iron saturation at the pole base (minimized by tapering)	$B_p \simeq 16$ KGauss
Total flux per pole	0.181 Wb
Flux dispersion	~ 33% of total flux
Ampereturns per pole	31500
Current	4500 A
Conductor current density	≤ 20 A/mm^2 max
Coil filling factor	~ 50 %
Voltage accross all coils in series	42 V
Overall power	189 KW
Water flow	190 l/min
Temperature rise	~ 15°C
Iron weight	~ 5100 Kg
Copper weight	~ 270 Kg
Overall magnet length	2200 mm

Fig. 2 shows a horizontal section through the pole. The side plates on which the pole piece sits are aluminum. Fig. 3 shows a side view of the magnet.

The performance of the magnet has been simulated by means of the CERN "Po-

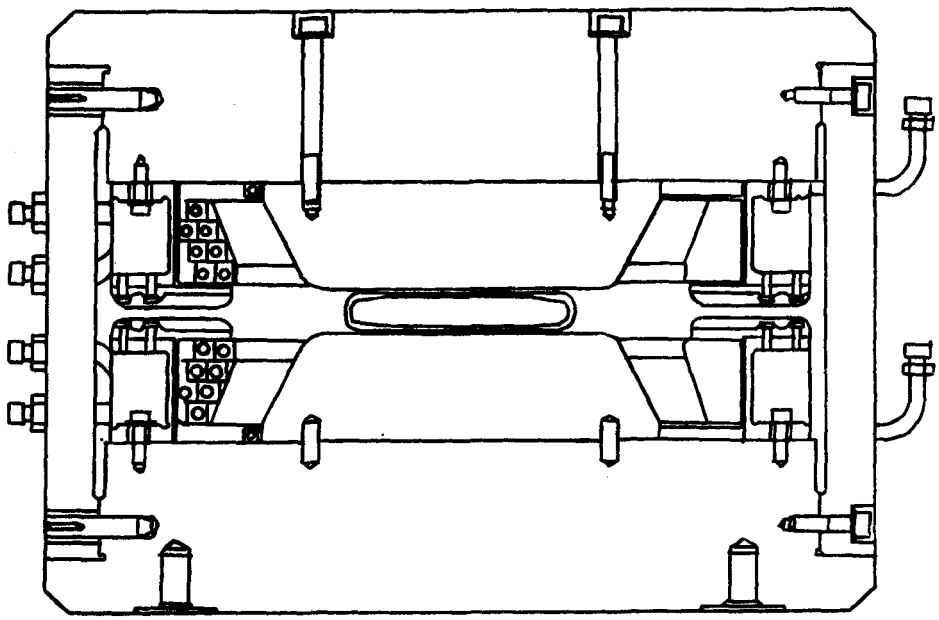

Fig.2.

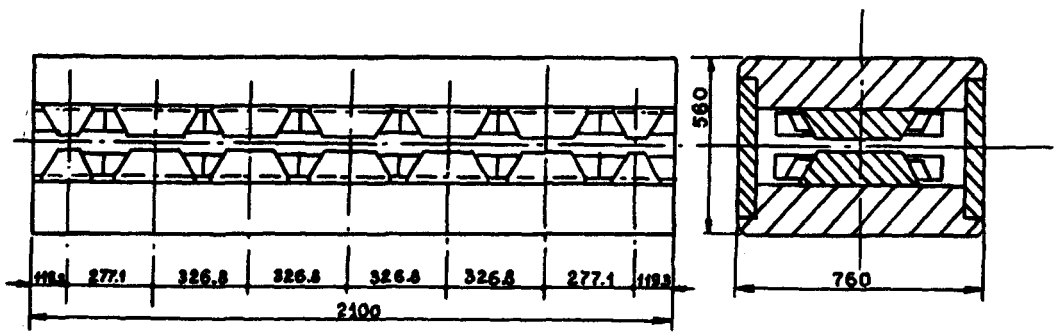

Fig.3.

isson" program and found to be quite satisfactory. Further work is in progress by means of three-dimensional mapping programs, to optimize details of the transverse useful aperture and longitudinal field integral.

The two end half-poles are equipped with an extra turn, providing a fine adjustement of the field integral via a separate small power supply. The existing MEA[4] compensator power supply allows the field integral to be corrected by as much as $\pm$ 60 G·m.

2. Effects on the machine optics

The insertion of a wiggler magnet in the lattice will of course modify the reference trajectory in the machine and, in general, all optical functions ($\beta_{x,z}$, η, $Q_{x,z}$, α_c). We will first deal with an ideal wiggler for which

$$\int B_z(s)\,ds = 0 \quad \text{and} \quad \frac{\partial B}{\partial x} = 0 \quad \text{for all } x,\ z, \tag{1}$$

and then estimate the tolerance on conditions (1).

It can be shown[5] that the perturbation matrices in the radial and the vertical plane for an ideal wiggler can be written as follows:

$$M_x = \begin{vmatrix} 1 & M_{12}^{(x)} & 0 \\ 0 & 1 & 0 \\ 0 & 0 & 1 \end{vmatrix}, \qquad M_z = \begin{vmatrix} \cos\theta^* & \beta^* \sin\theta^* \\ -\frac{1}{\beta^*}\sin\theta^* & \cos\theta^* \end{vmatrix}, \tag{2}$$

meaning that in the radial plane (x) the wiggler behaves like an additional straight section of length $M_{12}^{(x)}$, while in the vertical plane it behaves like a thin lens located at its center point. θ^* and β^* are functions of the radius of the curvature, ϱ_w, of particles in the wiggler.

The various parameters appearing in (2) have been calculated using the rectangular field model shown in Fig. 4.

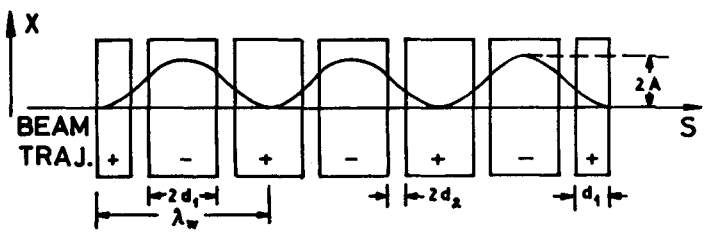

Fig. 4. Wiggler model ($d_1 + d_2 = d$).

For the proposed design one has:

- Equivalent length of a half-pole $d_1 = 11.82$ cm,
- Equivalent length of the straights in between poles $2d_2 = 9.04$ cm,
- Wiggler wavelength ($\lambda_w = 2(2d_1 + 2d_2)$) $\lambda_w = 65.36$ cm.

The radius of curvature in the wiggler is given, in the rectangular model, by

$$\varrho_w = p/eB_w \tag{3}$$

where p is the particle momentum and B_w the magnetic field in the wiggler.

The trajectory peak to peak amplitude, 2A, is given by

$$2A = \frac{\lambda_w^2}{16\varrho_w}\left(1 - \frac{d_2^2}{(d_1+d_2)^2}\right) . \tag{4}$$

Using the model of Fig. 4, it turns out[5] that

$$M_{12}^{(x)} = \frac{n\left[(d_1+d_2)^3 - d_2^2(d_2+3d_1)\right]}{\varrho_w^2} \simeq \frac{n(d_1+d_2)^3}{\varrho_w^2} \tag{5}$$

where n is twice the number of wavelengths in the wiggler.

In our case n = 6 so that

$$M_{12}^{(x)} \simeq 2.16 \text{ cm} . \tag{6}$$

This quantity is small enough that the motion in the horizontal plane is practically unaffected. Functions β_x and η are therefore changed by negligible amounts. The lengthening of the reference trajectory and the change in momentum compaction[5]

$$\Delta C \simeq \frac{M_{12}^{(x)}}{3} = .72 \text{ cm} , \qquad \frac{\Delta\alpha_c}{\alpha_c} \simeq -\frac{1}{\alpha_c}\frac{2n}{3}\frac{d}{L}\left(\frac{d}{\varrho_w}\right)^2 = 3.2\cdot 10^{-3} \tag{7}$$

(where $d = d_1+d_2$ and L is the overall orbit length) are also negligible .

To obtain a good match in the vertical plane one has to have

$$\beta^* = \beta_o \tag{8}$$

where β_o is the unperturbed value of β_z at the center of the wiggler, and compensate for θ^* by means of the machine quadrupoles. A plot of β^*, θ^* versus ϱ_w is given in Fig. 5.

It can be shown[5] that when $\varrho_w \to \infty$, β^* tends to a finite limit given by

$$\beta^*_{lim} \simeq \sqrt{\frac{(n^2-1)d^2}{3} + d_2^2} . \tag{9}$$

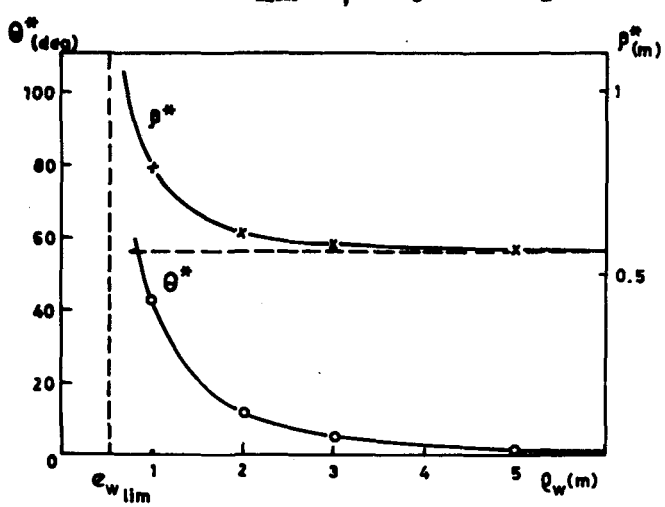

Fig. 5.

We choose to satisfy equation (8) by changing the machine operating point from $Q_x \simeq Q_z \simeq 3.1$ to $Q_x = 3.2$, $Q_z = 5.2$. At the latter point the value of β_o is

$$\beta_o(Q_z = 5.2) = .922$$

so that a satisfactory match is obtained around $\varrho_w \approx .8$ m. Of course for $\varrho_w \gg 1$m ϱ^* falls rapidly to zero so that the matching of β is no longer important.

In order to keep the horizontal closed orbit to within $\pm$ 2 mm, the construction tolerance on the field integral should not exceed $\sim$20 G·m. It is also required that the useful field region ($\Delta B/B \lesssim 10^{-3}$) be at least $\pm$110 mm at 10 KG and at least $\pm$60 mm at 18 KG in order to avoid undesirable quadrupole and higher order perturbations in the radial plane[5].

3. Effects on damping, momentum spread and beam emittances

Let us define the following integrals

$$I_m^{(w)} = \int_{L_w} \frac{ds}{|\varrho_w(s)|^m} \quad , \quad I_m^{(M)} = \int_{L_M} \frac{ds}{|\varrho_M|^m} \quad , \tag{10}$$

where L_w is the overall length of the wiggler, L_M that of the machine bending magnets, $\varrho_w(s)$ the local radius of curvature in the wiggler and ϱ_M the machine bending radius.

Since it can be shown that the damping partition coefficients are practically unaffected by the wiggler, the ratio of the perturbed to unperturbed damping time is given by[1,2]

$$\frac{\tau_w}{\tau_o} = \left(1 + \frac{I_2^{(w)}}{I_2^{(M)}}\right)^{-1} \quad , \tag{11}$$

and the perturbed to unperturbed momentum spread ratio is given by[1,2]

$$\left(\frac{\sigma_p}{\sigma_{p_o}}\right)^2 = \frac{1 + I_3^{(w)}/I_3^{(M)}}{1 + I_2^{(w)}/I_2^{(M)}} \quad . \tag{12}$$

In order to calculate the effect of the wiggler on the emittance it is necessary to know how the invariant H transforms . The invariant with wiggler, H, is related to that of the unperturbed machine, H_o, by formula[2]

$$\frac{H}{H_o} \cong \frac{1 + (I_3^{(w)}/I_3^{(M)})(\langle H_w \rangle / \langle H_o \rangle)}{1 + I_3^{(w)}/I_3^{(M)}} \quad , \tag{13}$$

where $\langle H_w \rangle$ is the invariant calculated over the wiggler magnetic field region. In evaluating (13) it should be kept in mind that, if $\varrho(s)$ varies appreciably along the integration path, terms $I_3\langle H \rangle$ in the numerator of (13) should be replaced by the exact formula[6]

$$I_3\langle H \rangle \rightarrow \int_{L_i} \frac{1}{\varrho^3(s)} (\alpha \eta^2 + 2\ \eta \eta' + \beta \eta'^2)\, ds \ . \tag{14}$$

Finally the ratio of perturbed to unperturbed emittances is given by

$$\frac{\varepsilon_{x\beta}}{\varepsilon_{x\beta_o}} = \frac{\varepsilon_z}{\varepsilon_{z_o}} = \frac{\sigma_p^2}{\sigma_{p_o}^2}\,\frac{H}{H_o} \simeq \frac{1 + (I_3^{(w)}/I_3^{(M)})\,(\langle H_w\rangle / \langle H_o\rangle)}{1 + I_2^{(w)}/I_2^{(M)}} \quad , \tag{15}$$

where $\varepsilon_{x\beta}$, $\varepsilon_{x\beta_o}$ are the betatron emittances in the radial plane.

The total radial emittance is of course given by

$$\varepsilon_x = \varepsilon_{x\beta} + \sigma_p^2 \eta^2 / \beta_x \quad . \tag{16}$$

Ratios (11), (12), (13), (15) are plotted versus ϱ_w, for our case, in Fig. 6a).

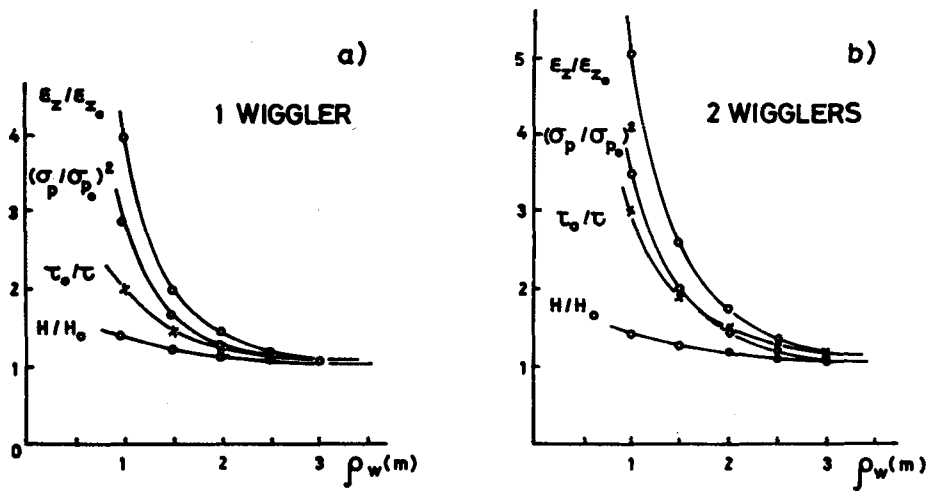

Fig. 6.

Fig. 6b.) shows the same quantities in the case where two identical wigglers are mounted on the machine. The use of two wigglers is envisaged for two-beam operation as explained in the following section.

The unperturbed values of emittance (ε_{x_o}, ε_{z_o}) at operating point $Q_x = 3.2$, $Q_z = 5.2$ are, in full coupling,

$$\varepsilon_{x_o} = 1.06 \cdot 10^{-7} \times E^2_{(GeV)} \text{ mrad} \quad , \quad \varepsilon_{z_o} = 4.6 \cdot 10^{-8} \times E^2_{(GeV)} \text{ mrad} \quad , \tag{17}$$

and are slightly lower than those at the normal operating point.

4. Colliding beams operation

It has been shown in sec. 3 that wigglers modify the beam emittance. In particular, in our case, the large increase in beam emittance for small values of ϱ_w, affords the possibility of increasing the storage ring luminosity at low energy.

In order however to be able to operate the ring in the colliding beam mode, two conditions have to be met:

a) the wiggler must be matched into the structure;

b) the phase shift in between two adjacent crossing regions must be the same for all crossings and must be equal to $(n+\delta)\pi$ with $\delta \ll 1$.

Condition a) means, as shown earlier, that the ring has to be operated at $Q_z = 5.2$. Condition b) requires the ring to be operated with one bunch per beam and with at least two wigglers, symmetrically placed with respect to the X-ing regions (due to the β^* introduced by each wiggler).

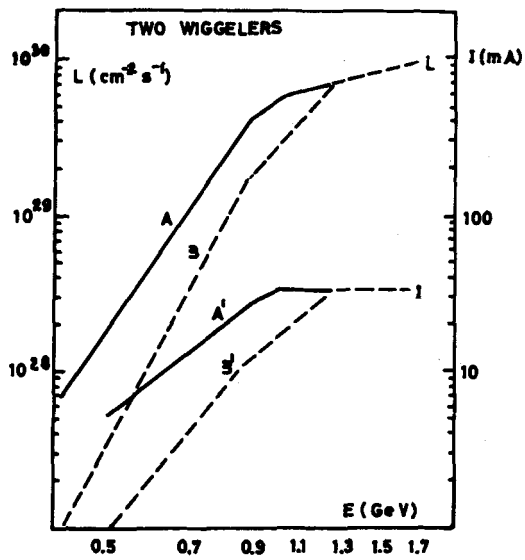

for $E > 884$ MeV $\quad \xi_{MAX} = 0.056$

$E < 884$ MeV $\quad \xi_{MAX} = 0.056(\frac{E}{884})^{1.5}$
(see ref. (7))

$I_{lim} = 33.3$ mA

A, A': wigglers on;

B, B': wigglers off.

Fig. 7.

Fig. 7 shows the expected behaviour of luminosity (curve A) and current per bunch (curve A') as a function of energy. The corresponding expected behaviours without wigglers, at the new operating point (3.2, 5.2) and with one bunch per beam, are also shown (curves B and B').

REFERENCES

1. M. Bassetti, Variable curvature function storage rings. Dimensions and damping control, T-66 INT. MEMO (1974); J. M. Paterson, J. R. Rees and H. Wiedemann, Control of beam size and polarization time in PEP, Report PEP-125/SPEAR-186 (1975).
2. A. Hutton, Control of the low energy characteristics of the LSR electron ring using wiggler magnets, Part. Acc. 7, 3 (1976).
3. H. Winick, Proc. Course on Synchrotron Radiation Research, Intern. College on Applied Physics, Alghero (1976), vol. I, pag. 1.
4. W. A. Ash et al., Description and performance of MEA, the magnetic detector at Adone, Frascati report LNF-77/18 (1977).
5. M. Bassetti, A. Cattoni, A. Luccio, M. Preger and S. Tazzari, A transverse wiggler magnet for Adone, Frascati report LNF-77/26 (1977).
6. M. Sands, The physics of electron storage rings. An introduction, Report SLAC-121 (1970).
7. F. Amman et al., Proc. VIIIth Intern. Conf. on High Energy Accelerators, CERN (1971).

ДИСКУССИЯ

R.Miller: If you put one small wiggler between every interaction point, couldn't you have multiple bunches in each beam?

A.Luccio: The answer is not immediate, because one has first to check whether the machine working point is suitable to match the wiggler into the lattice.